Journal of Scientific Computing, Vol. 8, No. 4, 1993

The Use of Richardson Extrapolation for the Numerical Solution of Low Mach Number Flow in Confined Regions

B. Christer V. Johansson[1]

Received November 20, 1992

We use artificial compressibility together with Richardson extrapolation in the Mach number M as a method for solving the time dependent Navier-Stokes equation for very low Mach number flow and for incompressible flow. The question of what boundary conditions one should use for low Mach number flow, especially at inflow and outflow boundaries, is investigated theoretically, and boundary layer suppressing boundary conditions are derived. For the case of linearization around a constant flow we show that the low Mach number solution will converge with the rate $O(M^2)$ to the true incompressible solution, provided that we choose the boundary conditions correctly. The results of numerical calculations for the time dependent, nonlinear equations and for flow situations with time dependent inflow velocity profiles are presented. The convergence rate M^2 to incompressible solution is numerically confirmed. It is also shown that using Richardson extrapolation to $M^2 = 0$ in order to derive a solution with very small divergence can with good result be carried through with M^2 as large as 0.1 and 0.05. As the time step in numerical methods must be chosen approximately such that $\Delta t \cdot (i/(M\,\Delta x) - \nu/\Delta x^2)$ is in the stability region of the time stepping method, and as $M^2 = 0.05$ is sufficiently small to yield good results, the restriction on the time step due to the Mach number is not serious. Therefore the equations can be integrated very fast by explicit time stepping methods. This method for solving very low Mach number flow and incompressible flow is well suited to parallel processing.

KEY WORDS: Navier-Stokes equations; incompressible; low Mach number; Richardson extrapolation; boundary layer; boundary condition; boundary layer suppressing boundary condition; inflow; outflow; open boundary.

[1] The Royal Institute of Technology, NADA-C2M2, S-100 44 Stockholm, Sweden. Present Address: Ericsson Radio Systems AB, Torshamnsgatan 23, S-164 80 Stockholm, Sweden.

854/8/4-1

1. INTRODUCTION

The use of artificial compressibility as a method to derive a solution of the Navier-Stokes equation for incompressible flow was first proposed by Chorin (1967). He used the equation

$$u_t + R((u^2)_x + (uv)_y) - u_{xx} - u_{yy} + p_x = 0 \tag{1.1a}$$

$$v_t + R((uv)_x + (v^2)_y) - v_{xx} - v_{yy} + p_y = 0 \tag{1.1b}$$

$$p_t + M^{-2} \cdot (u_x + v_y) = 0 \tag{1.1c}$$

where u and v are the velocities, p the pressure and R is the Reynolds number. Chorin (1967) called M^2 the artificial compressibility. In this article we will call M the artificial Mach number, or shortly the Mach number. If the solution of Eq. (1.1) converges to a steady state as $t \to \infty$, we see by Eq. (1.1c) that this solution is divergence free.

Kreiss *et al.* (1991) used another version of artificial compressibility, and investigated solutions of the equation

$$u_t + uu_x + vu_y - \nu(u_{xx} + u_{yy}) + p_x = 0 \tag{1.2a}$$

$$v_t + uv_x + vv_y - \nu(v_{xx} + v_{yy}) + p_y = 0 \tag{1.2b}$$

$$p_t + up_x + vp_y + M^{-2} \cdot (u_x + v_y) = 0 \tag{1.2c}$$

as $M \to 0$. They derived an asymptotic expansion in M^2 and showed convergence to an incompressible solution as $M^2 \to 0$. This was done both for the Cauchy problem and for an initial boundary value problem with simple inflow and outflow boundary conditions. The analysis revealed the existence of a boundary layer with the very small thickness νM^2 at the inflow boundary. They showed that prescribing u, v, and p as inflow boundary conditions will, as a function of M, make the boundary layer part of the solution $O(1)$ in p, $O(M^2)$ in u and $O(M^4)$ in v. In order to get rid of the $O(1)$ boundary layer they proposed to prescribe $u + aM^2 p$ $(a > u/2)$, v and $u_x + v_y$ at inflow. They showed that this will reduce the strength of the boundary layers to $O(M^2)$ in p, $O(M^4)$ in u and $O(M^6)$ in v.

Boundary conditions for the Navier-Stokes equation for incompressible flow were investigated by Naughton (1986) and Johansson (1991a–d). Naughton used the energy method to derive *a priori* estimates for the linearized problem together with inflow, outflow and solid wall boundary conditions.

Johansson (1991a,b) introduced the concept of boundary layer suppressing boundary conditions. Such conditions remove the boundary layer part of the solution by using normal derivatives of a high order. The

suppression of boundary layers at open boundaries is very important for two reasons. The first is that boundary layers at open boundaries are unphysical. The second is that if we, when solving the problem with numerical methods, do not suppress such layers, they must be resolved by making grid refinements. Otherwise they will cause wiggles in the numerical solution.

Boundary layer suppressing boundary conditions for open boundaries were derived by Johansson (1991a,b) for the Navier-Stokes equation for incompressible flow. Letting u be the velocity component normal and v the component tangential to the boundary, and letting $x=0$ be the boundary, the inflow boundary conditions

$$u(0, y, t) = u_0(y, t) \tag{1.3a}$$

$$\frac{\partial^r v}{\partial x^r}(0, y, t) = 0, \qquad r=0, \text{ or } r=1, \text{ or } r=2 \tag{1.3b}$$

$$\frac{\partial u}{\partial x}(0, y, t) + \frac{\partial v}{\partial y}(0, y, t) = 0 \tag{1.3c}$$

and the outflow boundary conditions

$$p(0, y, t) = p_0(y, t) \tag{1.4a}$$

$$\frac{\partial^j u}{\partial x^j}(0, y, t) = 0 \tag{1.4b}$$

$$\frac{\partial^k v}{\partial x^k}(0, y, t) = 0 \tag{1.4c}$$

were proposed. $r=2$, $j=3$, and $k=2$ were recommended. Theoretically and by numerical experiments, Johansson (1991a–d), the boundary conditions (1.3) and (1.4) were shown to

(i) suppress boundary layers at open boundaries,

(ii) give solutions that do not grow in time, if the forcing functions do not,

(iii) not produce divergence that can spread far into the domain, and

(iv) yield problems that are well-posed in the generalized sense, when the non-linear problem is linearized around an arbitrary smooth solution.

The aim of this article is to derive boundary conditions for the Eq. (1.2) such that (i)–(iv) is fulfilled and such that

(v) the low Mach number solution will, as $M \to 0$, converge with the rate $O(M^2)$ to the true incompressible solution, derived by Johansson (1991a,b).

We will not prove (iv) for the boundary conditions proposed in this article. However, the fact that the numerical calculations we carry through converge indicate that (iv) is fulfilled.

For the Eq. (1.2) we in this article suggest the inflow boundary conditions

$$u(0, y, t) = u_0(y, t) \tag{1.5a}$$

$$\frac{\partial^r v}{\partial x^r}(0, y, t) = 0, \qquad r = 0, \text{ or } r = 1, \text{ or } r = 2 \tag{1.5b}$$

$$\frac{\partial^q u}{\partial x^q}(0, y, t) = 0, \qquad q \geqslant 2 \tag{1.5c}$$

the outflow boundary conditions

$$p(0, y, t) = p_0(y, t) \tag{1.6a}$$

$$\frac{\partial^k v}{\partial x^k}(0, y, t) = 0, \qquad k \geqslant 1 \tag{1.6b}$$

and the solid wall boundary conditions

$$u(0, y, t) = 0 \tag{1.7a}$$

$$\frac{\partial^r v}{\partial x^r}(0, y, t) = 0, \qquad r = 0 \text{ or } r = 1 \tag{1.7b}$$

Again, for all the conditions in Eqs. (1.5)–(1.7), u is the velocity component normal to the boundary. For Eq. (1.5) we recommend to use $r = 2$ and $q = 3$. For Eq. (1.6) we recommend to use $k = 2$. Using $r = 0$ in Eq. (1.7) yields the no slip condition, and $r = 1$ yields the slip condition.

The generalization of these boundary conditions to three dimensions is straight forward. At each boundary we will need one more condition, and this is formed by treating the third velocity component in the same way as we treat v.

For the case of linearization around a constant flow we theoretically show that the boundary conditions Eqs. (1.5) and (1.6) yield solutions that fulfill (i) and (v), at least for the steady state solution. At the inflow boundary we will get two sets of boundary layers, one with the thickness νM^2 and one with the thickness $|\omega|^{-1}$, where $|\omega|^{-1}$ is the typical length scale for variations of the inflow profile $u_0(y, t)$. The $|\omega|^{-1}$-boundary layer was

discovered by Johansson (1991a,b). The boundary layer with thickness νM^2 is the one that was discovered in Kreiss *et al.* (1991). As by Johansson (1991a,b) we suppress the $|\omega|^{-1}$-boundary layer by choosing r large in Eq. (1.5b). However, as shown by Johansson (1991a,b) using $r \geqslant 3$ will make it impossible to get (ii) fulfilled for the incompressible case, and we therefore recommend to use $r = 2$. The νM^2-boundary layer will, as a function of ν and M, have the magnitude $O(\nu^{\min+q} M^{2q})$ in u, $O(\nu^{\min+q+1} M^{2q+2})$ in v and $O(\nu^{\min+q} M^{2q-2})$ in p. Here $\min = \min(r+1, q)$, and r and q are given in Eq. (1.5). Hence, this boundary layer can be suppressed to any order by choosing q large enough. This is a considerable improvement compared to using the boundary conditions proposed by Kreiss *et al.* (1991). The restriction $q \geqslant 2$ is necessary in order to get the condition (v) fulfilled. This means that it is necessary to suppress the νM^2-boundary layer properly, in order to get convergence to the true incompressible solution as $M \to 0$. We recommend to use $q = 3$.

As in the incompressible case, Johansson (1991a,b), we get a boundary layer with thickness ν at the outflow boundary. The larger the k we use in Eq. (1.6b), the more suppressed this boundary layer will be. We recommend to use $k = 2$.

We solve the nonlinear time-dependent Eq. (1.2) together with Eq. (1.5) at the inflow, Eq. (1.6) at the outflow and Eq. (1.7) at the solid wall boundary numerically and show that (i)–(iii) and (v) hold for this case as well. Especially, the divergence in the solution is $O(M^2)$.

The existence of an asymptotic expansion in M^2, Kreiss *et al.* (1991), shows that applying Richardson extrapolation to $M^2 = 0$ yields a solution which divergence is $O(M^4)$. We confirm this numerically. We also show that it is sufficient to make one calculation with $M^2 = 0.1$ and one with $M^2 = 0.05$ and using Richardson extrapolation to $M^2 = 0$ in order to derive a solution with very small divergence.

The time step Δt in the numerical method must be chosen approximately such that $\Delta t \cdot (i/(M\,\Delta x) - \nu/\Delta x^2)$ is in the stability region of the method. As using $M^2 = 0.1$ and $M^2 = 0.05$ yields very good result, the restriction on the time step for explicit methods due to the Mach number is not serious. Hence, approximating spatial derivatives in Eq. (1.2) with finite differences, integrating in time with an explicit method for two moderate values of M^2, and applying Richardson extrapolation to $M^2 = 0$ or to a very small value of M^2, is a very effective method for solving time-dependent incompressible flow problems and very low Mach number flow problems. As the method uses finite differences in space and explicit time integration, it is very well suited to parallel processing.

The rest of this article is arranged as follows. Note that Section 6 can be read independently of the preceding sections.

In Section 2, we by linearizing the Eq. (1.2) around a constant flow derive a model problem for investigating boundary conditions.

In Section 3, we derive the number of boundary conditions required at different types of boundaries. In Section 3.1 we take the Laplace-Fourier transform of the linearized problem and derive the fundamental solution. In Section 3.2, we prove that in order to get the solution well defined we must apply three boundary conditions at the inflow boundary, two conditions at the outflow boundary, and two conditions at boundaries through which no fluid passes.

In Section 4, we derive the boundary layer suppressing boundary conditions Eq. (1.5) for inflow and Eq. (1.6) for outflow. In order to simplify the algebra we restrict the investigation to steady state. In Section 4.1, we identify the boundary layer part of the fundamental solution derived in Section 3.1. In Section 4.2, we show that the boundary conditions Eqs. (1.5) and (1.6) suppress boundary layers and that the low Mach number solution converges with the rate $O(M^2)$ to the true incompressible solution as $M^2 \to 0$.

In Section 5, we consider the no slip and the slip conditions Eq. (1.7) for boundaries through which no fluid passes.

In Section 6, we present numerical solutions of the Eq. (1.2) in a two dimensional straight channel. We use the boundary conditions Eq. (1.5) with $r=2$ and $q=3$, Eq. (1.6) with $k=2$ and Eq. (1.7) with $r=0$. We show the uniform convergence to the incompressible solution as $M^2 \to 0$. We also show that making one calculation with $M^2=0.1$ and one with $M^2=0.05$ and applying Richardson extrapolation to $M^2=0$ yields a solution with very small divergence. The calculations are carried through both for flows that approaches steady state and for flows with inflow velocity profiles $u_0(y, t)$ that are periodic in t.

2. A MODEL PROBLEM FOR OPEN BOUNDARIES: THE LINEARIZATION AROUND A CONSTANT FLOW

In this article we will consider the Eq. (1.2), especially for small Mach numbers. The restriction to two space dimensions is no real restriction, as we could treat the z-direction in the same way as the y-direction. The result of the analysis in three dimensions is that we at each boundary must prescribe one extra boundary condition, and that this boundary condition can be formed by treating the third velocity component in the same way as we treat the v-component.

In order to investigate boundary conditions, we linearize the Eq. (1.2) around a constant flow (U, V, P). We let the domain be $0 \leqslant x < \infty$, $0 \leqslant y \leqslant 2\pi$, $0 \leqslant t < \infty$. Hence, we let $(u, v, p) = (U+u', V+v', P+p')$

where the perturbation (u', v', p') is small. Omitting the primes, the perturbation approximately fulfills the equation

$$u_t + Uu_x + Vu_y - \nu(u_{yy} + u_{xx}) + p_x = 0, \quad 0 \leqslant x < \infty,\ 0 \leqslant y \leqslant 2\pi,\ 0 \leqslant t < \infty \tag{2.1a}$$

$$v_t + Uv_x + Vv_y - \nu(v_{yy} + v_{xx}) + p_y = 0, \quad 0 \leqslant x < \infty,\ 0 \leqslant y \leqslant 2\pi,\ 0 \leqslant t < \infty \tag{2.1b}$$

$$p_t + Up_x + Vp_y + M^{-2} \cdot (u_x + v_y) = 0, \quad 0 \leqslant x < \infty,\ 0 \leqslant y \leqslant 2\pi,\ 0 \leqslant t < \infty \tag{2.1c}$$

As we will take a special interest in low Mach number flow and in the incompressible limit $M \to 0$, we will assume that $1/(1 - U^2M^2)$ is at most $O(1)$. This can for instance be fulfilled by assuming that

$$U^2M^2 < \tfrac{1}{2}$$

We apply boundary conditions at $x = 0$ and require the solution to be 2π-periodic in the y-direction. The boundary condition at $x = 0$ is written as

$$B(\partial/\partial x, \partial/\partial y, \partial/\partial t)\begin{pmatrix} u \\ v \\ p \end{pmatrix} = g(y, t), \qquad x = 0, \quad 0 \leqslant y \leqslant 2\pi, \quad 0 \leqslant t < \infty \tag{2.1d}$$

where B is a differential operator with constant coefficients. B can be for instance 1 (Dirichlet condition) or $\partial/\partial x$ (Neumann condition). We consider a simple class of forcing functions g and for simplicity demand that $g \in C^\infty$ and that g and all its derivatives vanish identically at $t = 0$.

The solution must vanish at $x = \infty$, and we therefore as a side condition demand that

$$\int_0^\infty e^{-2\eta t}(\|u(\cdot, \cdot, t)\|^2 + \|v(\cdot, \cdot, t)\|^2 + \|p(\cdot, \cdot, t)\|^2)\, dt < \infty, \qquad \eta > \eta_0 \tag{2.1e}$$

for some $\eta_0 \in R$. Here $\|h(\cdot, \cdot, t)\|$ is the L_2-norm of h, that is $\|h(\cdot, \cdot, t)\|^2 = \int_0^\infty \int_0^{2\pi} h^2\, dy\, dx$.

Equation (2.1e) can be considered as a boundary condition at $x = \infty$. The reason that we use the condition Eq. (2.1e) and not for instance $\begin{pmatrix} u \\ v \\ p \end{pmatrix} \to 0$ as $x \to \infty$, is that if we use Eq. (2.1e) as the side condition we can use Parseval's relation to derive a side condition for the Laplace-Fourier transform of $\begin{pmatrix} u \\ v \\ p \end{pmatrix}$.

As initial condition we let

$$\begin{pmatrix} u \\ v \\ p \end{pmatrix}(x, y, 0) = 0, \qquad 0 \leqslant x < \infty, \qquad 0 \leqslant y \leqslant 2\pi \tag{2.1f}$$

3. SOLUTION VIA THE LAPLACE-FOURIER TRANSFORM

3.1. The Fundamental Solution

We start with defining some notations. For a function $h = h(x, y, t)$ the Laplace-Fourier transform, for $\text{Real}(s) = \eta \geqslant \eta_0$ and for $\omega \in Z$, is defined by

$$\hat{h}(x, \omega, s) = \frac{1}{2\pi} \int_0^{2\pi} \int_0^{\infty} e^{-st} e^{-i\omega y} h(x, y, t)\, dt\, dy$$

The inverse Laplace-Fourier transform is

$$h(x, y, t) = \frac{1}{2\pi i} \int_{\eta - i\infty}^{\eta + i\infty} \sum_{\omega = -\infty}^{\infty} e^{st} e^{i\omega y} \hat{h}(x, \omega, s)\, ds$$

We define the L_2-norm of $\hat{h}$ as $\|\hat{h}(\cdot, \cdot, s)\|^2 = \sum_{\omega = -\infty}^{\infty} \int_0^{\infty} |\hat{h}(x, \omega, s)|^2\, dx$, and Parseval's relation yields

$$\int_0^{\infty} e^{-2\eta t} \|h(\cdot, \cdot, t)\|^2\, dt = \int_{-\infty}^{\infty} \|\hat{h}(\cdot, \cdot, \eta + i\xi)\|^2\, d\xi$$

Taking the Laplace-Fourier transform of the problem Eq. (2.1) yields

$$s\hat{u} + U\hat{u}_x + i\omega V\hat{u} - \nu\hat{u}_{xx} + \nu\omega^2\hat{u} + \hat{p}_x = 0, \quad 0 \leqslant x < \infty, \ \omega \in Z \tag{3.1a}$$

$$s\hat{v} + U\hat{v}_x + i\omega V\hat{v} - \nu\hat{v}_{xx} + \nu\omega^2\hat{v} + i\omega\hat{p} = 0, \quad 0 \leqslant x < \infty, \ \omega \in Z \tag{3.1b}$$

$$s\hat{p} + U\hat{p}_x + i\omega V\hat{p} + M^{-2} \cdot (\hat{u}_x + i\omega\hat{v}) = 0, \quad 0 \leqslant x < \infty, \ \omega \in Z \tag{3.1c}$$

$$B(\partial/\partial x, i\omega, s) \begin{pmatrix} \hat{u} \\ \hat{v} \\ \hat{p} \end{pmatrix} = \hat{g}(\omega, s), \qquad x = 0, \quad \omega \in Z \tag{3.1d}$$

$$\int_{-\infty}^{\infty} (\|\hat{u}(\cdot, \cdot, \eta + i\xi)\|^2 + \|\hat{v}(\cdot, \cdot, \eta + i\xi)\|^2 + \|\hat{p}(\cdot, \cdot, \eta + i\xi)\|^2)\, d\xi < \infty, \qquad \eta > \eta_0 \tag{3.1e}$$

In order to solve Eq. (3.1) we make the *ansatz*

$$\begin{pmatrix} \hat{u} \\ \hat{v} \\ \hat{p} \end{pmatrix}(x, \omega, s) = \begin{pmatrix} \hat{u} \\ \hat{v} \\ \hat{p} \end{pmatrix}(0, \omega, s) \cdot e^{-\kappa(\omega, s)x}$$

and Eqs. (3.1a–c) becomes

$$A \cdot \begin{pmatrix} \hat{u} \\ \hat{v} \\ \hat{p} \end{pmatrix}(0, \omega, s) = \begin{pmatrix} 0 \\ 0 \\ 0 \end{pmatrix} \tag{3.2a}$$

$$A = \begin{pmatrix} s - U\kappa + i\omega V - \nu\kappa^2 + \nu\omega^2 & 0 & -\kappa \\ 0 & s - U\kappa + i\omega V - \nu\kappa^2 + \nu\omega^2 & i\omega \\ -M^{-2}\kappa & M^{-2} i\omega & s - U\kappa + i\omega V \end{pmatrix} \tag{3.2b}$$

Equation (3.2) has nontrivial solutions only if the determinant of the matrix A is zero, i.e. if

$$\kappa^2 + \frac{U}{\nu}\kappa - \frac{s + i\omega V + \nu\omega^2}{\nu} = 0 \tag{3.3a}$$

or

$$\begin{aligned} U\nu \cdot \kappa^3 + (U^2 - \nu(s + i\omega V) - M^{-2}) \cdot \kappa^2 - U(2s + 2i\omega V + \nu\omega^2) \cdot \kappa \\ + (s + i\omega V)(s + i\omega V + \nu\omega^2) + M^{-2}\omega^2 = 0 \end{aligned} \tag{3.3b}$$

The two roots of Eq. (3.3a) will be denoted κ_{a1} and κ_{a2}. For $U \neq 0$ Eq. (3.3b) has three roots which will be denoted κ_{b1}, κ_{b2} and κ_{b3}. The eigenvectors corresponding to these roots are

$$e_{aj} = \begin{pmatrix} 1 \\ \dfrac{\kappa_{aj}}{i\omega} \\ 0 \end{pmatrix}, \qquad j = 1, 2$$

and

$$e_{bj} = \begin{pmatrix} 1 \\ \dfrac{-i\omega}{\kappa_{bj}} \\ \dfrac{s - \kappa_{bj}U + i\omega V - \nu\kappa_{bj}^2 + \nu\omega^2}{\kappa_{bj}} \end{pmatrix}, \qquad j = 1, 2, 3$$

The expression for e_{aj} above is only valid for $\omega \neq 0$. For $\omega = 0$ the $\hat{v}$-equation Eq. (3.1b) is decoupled from the $\hat{u}$- and $\hat{p}$-equations Eqs. (3.1a) and (3.1c), and we have $e_{aj} = \begin{pmatrix} 0 \\ 1 \\ 0 \end{pmatrix}$. As we will focus the theoretical investigation in Sections 3 and 4 on deriving boundary layer suppressing boundary conditions for open boundaries, we from here on only consider the case $\omega \neq 0$.

The fundamental solution of Eq. (3.1) is derived by forming the linear combination of the eigensolutions. For $\omega \neq 0$ and $U \neq 0$ we get

$$\begin{pmatrix} \hat{u} \\ \hat{v} \\ \hat{p} \end{pmatrix} = \sum_{j=1}^{2} \alpha_{aj} \begin{pmatrix} 1 \\ \dfrac{\kappa_{aj}}{i\omega} \\ 0 \end{pmatrix} \cdot e^{-\kappa_{aj} x} + \sum_{j=1}^{3} \alpha_{bj} \begin{pmatrix} 1 \\ \dfrac{-i\omega}{\kappa_{bj}} \\ \dfrac{s - \kappa_{bj} U + i\omega V - \nu \kappa_{bj}^2 + \nu\omega^2}{\kappa_{bj}} \end{pmatrix} e^{-\kappa_{bj} x} \tag{3.4}$$

For $\omega \neq 0$ and $U = 0$ the root κ_{b3} disappears, and the second summation will only be carried through from $j = 1$ to $j = 2$.

3.2. The Number of Boundary Conditions

The α:s in Eq. (3.4) that belong to the κ:s with a negative real part disappear due to the side condition Eq. (3.1e). The remaining α:s must be determined by the boundary condition at $x = 0$. Hence, the number of boundary conditions at $x = 0$ must equal the number of κ:s with a positive real part. It is therefore very important to determine this number. The result of the investigation in Section 3.2 is that we must prescribe three conditions at inflow boundaries, two at outflow boundaries and two at boundaries through which no fluid passes. In three dimension we at each boundary must prescribe one more condition.

The solution of Eq. (3.3a) is

$$\kappa_{a1} = -\frac{U}{2\nu} + \sqrt{\frac{U^2}{4\nu^2} + \omega^2 + \frac{s + i\omega V}{\nu}} \tag{3.5a}$$

and

$$\kappa_{a2} = -\frac{U}{2\nu} - \sqrt{\frac{U^2}{4\nu^2} + \omega^2 + \frac{s + i\omega V}{\nu}} \tag{3.5b}$$

For $\text{Real}(s) > -\nu\omega^2$ we see that $\text{Real}(\kappa_{a1}) > 0$ and $\text{Real}(\kappa_{a2}) < 0$.

The signs of the real parts of the roots of Eq. (3.3b) are given in Theorem 3.1. As a preparation for the proof of Theorem 3.1, we have the following Lemma.

Lemma 3.1. Let $\text{Real}(s) > \max(-v\omega^2/2, -v^{-1}M^{-2})$. Then Eq. (3.3b) has no root κ on the imaginary axis.

Proof of Lemma 3.1. Let $\text{Real}(s) = \eta$, let $\text{Im}(s + i\omega V) = \xi$ and assume that $\kappa = ik$ where $k \in R$. The imaginary part of Eq. (3.3b) then becomes

$$-Uv \cdot k^3 + v\xi \cdot k^2 - U(2\eta + v\omega^2) \cdot k + \xi(2\eta + v\omega^2) = 0 \qquad (3.6a)$$

and the real part becomes

$$-(U^2 - v\eta - M^{-2}) \cdot k^2 + 2U\xi \cdot k + (\eta^2 - \xi^2 + v\omega^2\eta + M^{-2}\omega^2) = 0 \qquad (3.6b)$$

For $U \neq 0$ Eq. (3.6a) has the roots

$$k_{1,2} = \pm i \sqrt{\frac{2\eta}{v} + \omega^2}$$

$$k_3 = \frac{\xi}{U}$$

As $2\eta/v + \omega^2 > 0$ by assumption, we have $k_{1,2} \notin R$. Hence the only $k \in R$ that solves Eq. (3.6a) is ξ/U. However, letting $k = \xi/U$ and making use of the assumption $\eta > -v^{-1}M^{-2}$ yields for the left-hand side of Eq. (3.6b)

$$\begin{aligned}\text{left-hand side} = &-(U^2 - v\eta - M^{-2}) \cdot \left(\frac{\xi}{U}\right)^2 + 2\xi U \cdot \frac{\xi}{U} \\ &+ \eta^2 - \xi^2 + v\omega^2\eta + M^{-2}\omega^2 \\ &= \eta^2 + (v\eta + M^{-2}) \cdot (\omega^2 + \xi^2 U^{-2}) > 0\end{aligned}$$

Therefore Eq. (3.6b) is not fulfilled, and for $U \neq 0$ Eq. (3.3b) has no root κ on the imaginary axis.

Now consider the case $U = 0$. As $\eta > -v\omega^2/2$ by assumption, Eq. (3.6a) for $U = 0$ is only fulfilled if $\xi = 0$. Letting $\xi = 0$ and making use of the assumption $\eta > -v^{-1}M^{-2}$ yields for the left-hand side of Eq. (3.6b)

$$\text{left-hand side} = \eta^2 + (v\eta + M^{-2}) \cdot (k^2 + \omega^2) > 0$$

Therefore Eq. (3.6b) is not fulfilled, and for $U = 0$ Eq. (3.3b) has no root κ on the imaginary axis.

The proof of Lemma 3.1 is complete. ◆

We next calculate the number of roots of Eq. (3.3b) that have a positive real part, and the number that has a negative real part. As the roots of Eq. (3.3b) are continuous functions of s, and as there are no roots on the imaginary axis, we only need to consider $\text{Real}(s) = \eta \in R$ for large η. We will use Rouché's Theorem, [e.g., Dettman (1984)], that says that if $f = f(\kappa)$ and $g = g(\kappa)$ are analytic on and inside a simple closed contour Γ, if $|g(\kappa)/f(\kappa)| < 1$ on Γ and if $f(\kappa) \neq 0$ on Γ, then $f(\kappa)$ and $f(\kappa) + g(\kappa)$ has the same number of zeros inside Γ.

Theorem 3.1. If $\text{Real}(s) > \max(-v\omega^2/2, -v^{-1}M^{-2})$ the following is true:

For $U > 0$, Eq. (3.3b) has two roots κ with $\text{Real}(\kappa) > 0$ and one root κ with $\text{Real}(\kappa) < 0$.

For $U < 0$, Eq. (3.3b) has one root κ with $\text{Real}(\kappa) > 0$ and two roots κ with $\text{Real}(\kappa) < 0$.

For $U = 0$, Eq. (3.3b) has one root κ with $\text{Real}(\kappa) > 0$ and one root κ with $\text{Real}(\kappa) < 0$.

Proof. We first consider the case $U \neq 0$. Let $\text{Real}(s) = \eta > \max(-v\omega^2/2, -v^{-1}M^{-2})$ and $\text{Im}(s) = -\omega V$. Equation (3.3b) then becomes

$$\kappa^3 + \frac{U^2 - v\eta - M^{-2}}{vU}\kappa^2 - \frac{2\eta + v\omega^2}{v}\kappa + \frac{\eta(\eta + v\omega^2) + M^{-2}\omega^2}{vU} = 0$$

Let

$$f(\kappa) = \frac{U^2 - v\eta - M^{-2}}{vU}\kappa^2 + \frac{\eta(\eta + v\omega^2) + M^{-2}\omega^2}{vU}$$

$$g(\kappa) = \kappa^3 - \frac{2\eta + v\omega^2}{v}\kappa$$

and let the contour Γ be either of the circles

$$\kappa = \pm\left(\frac{\eta(\eta + v\omega^2) + M^{-2}\omega^2}{M^{-2} + v\eta - U^2}\right)^{1/2} + \frac{|U|}{v} \cdot e^{i\varphi}, \qquad 0 \leqslant \varphi \leqslant 2\pi$$

This yields for η large enough

$$\left|\frac{g(\kappa)}{f(\kappa)}\right| = \left|\frac{\kappa\left(\kappa^2 - \dfrac{2\eta + v\omega^2}{v}\right)}{\dfrac{U^2 - v\eta - M^{-2}}{vU}\kappa^2 + \dfrac{\eta(\eta + v\omega^2) + M^{-2}\omega^2}{vU}}\right| = \frac{1}{2} + O(\eta^{-1/2}) < 1$$

By Rouché's Theorem $g+f$ has one zero inside the circle

$$\kappa = \left(\frac{\eta(\eta + \nu\omega^2) + M^{-2}\omega^2}{M^{-2} + \nu\eta - U^2} \right)^{1/2} + \frac{|U|}{\nu} e^{i\varphi}$$

and one zero inside the circle

$$\kappa = -\left(\frac{\eta(\eta + \nu\omega^2) + M^{-2}\omega^2}{M^{-2} + \nu\eta - U^2} \right)^{1/2} + \frac{|U|}{\nu} e^{i\varphi}$$

In the same way it is shown that the third root is inside the circle

$$\kappa = -\frac{U^2 - \nu\eta - M^{-2}}{\nu U} + \frac{2\,|U|}{\nu} e^{i\varphi}$$

Hence, for $\eta = \text{Real}(s)$ large enough, the three roots of Eq. (3.3b) are

$$\kappa_{b1} = \left(\frac{\eta(\eta + \nu\omega^2) + M^{-2}\omega^2}{M^{-2} + \nu\eta - U^2} \right)^{1/2} + O(U/\nu) = \left(\frac{\eta}{\nu} \right)^{1/2} (1 + O(\eta^{-1/2})) \tag{3.7a}$$

$$\kappa_{b2} = -\left(\frac{\eta(\eta + \nu\omega^2) + M^{-2}\omega^2}{M^{-2} + \nu\eta - U^2} \right)^{1/2} + O(U/\nu) = -\left(\frac{\eta}{\nu} \right)^{1/2} (1 + O(\eta^{-1/2})) \tag{3.7b}$$

and

$$\kappa_{b3} = -\frac{U^2 - \nu\eta - M^{-2}}{\nu U} + O(U/\nu) = \frac{\eta}{U} (1 + O(\eta^{-1})) \tag{3.7c}$$

We next consider $U = 0$. In this case the roots of Eq. (3.3b) are

$$\kappa_{b1} = \left(\frac{\eta}{\nu} \right)^{1/2} (1 + O(\eta^{-1})) \tag{3.8a}$$

$$\kappa_{b2} = -\left(\frac{\eta}{\nu} \right)^{1/2} (1 + O(\eta^{-1})) \tag{3.8b}$$

As the roots of Eq. (3.3b) are continuous functions of s, Theorem 3.1 follows from Lemma 3.1 and the expressions in Eqs. (3.7) and (3.8). ◆

4. BOUNDARY LAYER SUPPRESSING CONDITIONS FOR OPEN BOUNDARIES

In this section we will derive inflow and outflow boundary conditions for the Navier-Stokes equation for low Mach number flow, formulated as

Eq. (1.2). The aim is to find boundary conditions such that boundary layers at open boundaries are suppressed, and such that the low Mach number solution converges to the true incompressible solution, derived in Johansson (1991a,b), as $M \to 0$.

We will use the fact that boundary layers at open boundaries are unphysical. This can be used to formulate a criterion for good boundary conditions for open boundaries, Johansson (1991a,b):

> *A boundary condition for an open boundary is good if it has the property of suppressing boundary layers.*

In order to simplify the algebra we will in Section 4 assume that $V = 0$ and $s = 0$. Considering $s = 0$ means that we restrict the theoretical investigation to the case of steady state.

A more careful investigation would involve all s to the right of a line $\text{Real}(s) = \eta_0$. If there is a unique solution of Eq. (3.1) that is analytic in the domain $\text{Real}(s) > \eta_0$, and if this solution decays fast enough as $|\omega| \to \infty$ and as $s \to \infty$ in this domain, the inverse Laplace-Fourier transform exists and solves the original problem Eq. (2.1), [Gustafsson *et al.* (1990); Johansson (1991a–d); and Kreiss *et al.* (1989)]. In this section we will assume the existence of such a solution, and concentrate on the question of finding boundary layer suppressing boundary conditions. This assumption will be justified by the numerical experiments shown in Section 6. These experiments are carried through with the original nonlinear and time dependent Eq. (1.2).

As in Johansson (1991a,b), we start by determining the relative magnitude of the κ:s.

4.1. The Relative Magnitude of the κ:s for $s = 0$

For the simplifications made above Eq. (3.3b) becomes

$$\kappa^3 + \frac{U^2 - M^{-2}}{vU}\kappa^2 - \omega^2 \cdot \kappa + \frac{M^{-2}\omega^2}{vU} = 0 \tag{4.1}$$

where $1/(1 - U^2M^2)$ is at most $O(1)$. We have the following theorem.

Theorem 4.1. For $|\omega v U M^2| \gg 1$ the zeros of Eq. (4.1) are

$$\kappa_{b1} = |\omega| \left(1 + O\left(\frac{U}{\omega v}\right)\right)$$

$$\kappa_{b2} = -|\omega| \left(1 + O\left(\frac{U}{\omega v}\right)\right)$$

$$\kappa_{b3} = \frac{1}{UvM^2}\left(1 + O\left(\frac{1}{\omega^2 v^2 M^2}\right)\right)$$

For $|\omega v U M^2| \ll 1$ the zeros of Eq. (4.1) are

$$\kappa_{b1} = \frac{|\omega|}{(1-U^2M^2)^{1/2}}(1 + O(\omega v U^3 M^4))$$

$$\kappa_{b2} = -\frac{|\omega|}{(1-U^2M^2)^{1/2}}(1 + O(\omega v U^3 M^4))$$

$$\kappa_{b3} = \frac{1-U^2M^2}{UvM^2}(1 + O(\omega^2 v^2 U^4 M^6))$$

For $|\omega U v M^2| = O(1)$, all roots are at most $O(|\omega|)$.

Proof. We rescale Eq. (4.1) by letting

$$m = |\omega|\, vUM^2 \tag{4.2}$$

and

$$\beta = \frac{\kappa}{|\omega|} \tag{4.3}$$

which in Eq. (4.1) gives

$$\beta^3 - \frac{1-U^2M^2}{m}\beta^2 - \beta + \frac{1}{m} = 0 \tag{4.4}$$

First consider $|m| = |\omega v U M^2| \gg 1$ and let

$$f(\beta) = \beta^3 - \beta$$

$$g(\beta) = -\frac{1-U^2M^2}{m}\beta^2 + \frac{1}{m}$$

and

$$\beta = 1 + \frac{U^2M^2}{|m|}\cdot e^{i\varphi}$$

This gives

$$\left|\frac{g(\beta)}{f(\beta)}\right| = \left|\frac{-\dfrac{1-U^2M^2}{m}\beta^2 + \dfrac{1}{m}}{\beta^3 - \beta}\right| = \frac{1}{2}(1 + O(|m|^{-1})) < 1$$

By Rouché's Theorem, Eq. (4.4) has one root inside $\beta = 1 + U^2M^2/|m| \cdot e^{i\varphi}$, i.e. Eq. (4.1) has one root inside $\kappa = |\omega| + U/v \cdot e^{i\varphi}$, and the first expression for κ_{b1} in Theorem 4.1 follows.

The other expressions for κ_{b1}, κ_{b2} and κ_{b3} follows in the same way.

Finally we consider the case $|\omega|\ vUM^2 = O(1)$. As the coefficients in Eq. (4.4) are $O(1)$ for $m = O(1)$, the roots of Eq. (4.4) are at most $O(1)$ as well, i.e. the roots of Eq. (4.1) are at most $O(|\omega|)$.

The proof of Theorem 4.1 is complete. ◆

4.2. The Suppression of Boundary Layers and the Convergence to the Incompressible Solution

We will now prescribe boundary conditions at $x = 0$ such that

(i) the α:s in Eq. (3.4) will be uniquely determined,

(ii) the boundary layer part of the solution will be suppressed, and

(iii) the low Mach number solution will, as $M \to 0$, converge with the rate $O(M^2)$ to the true incompressible solution, derived in Johansson (1991a,b).

As an example we will carry through the investigation for $|v\omega| \ll 1$. We start with inflow.

4.2.1. Inflow

4.2.1.1. The Boundary Condition. (See Fig. 1). Choosing $U > 0$ makes $x = 0$ an inflow boundary. Furthermore, $U > 0$ implies that κ_{a1}, κ_{b1} and κ_{b3} have a strictly positive real part, whereas κ_{a2} and κ_{b2} have a strictly

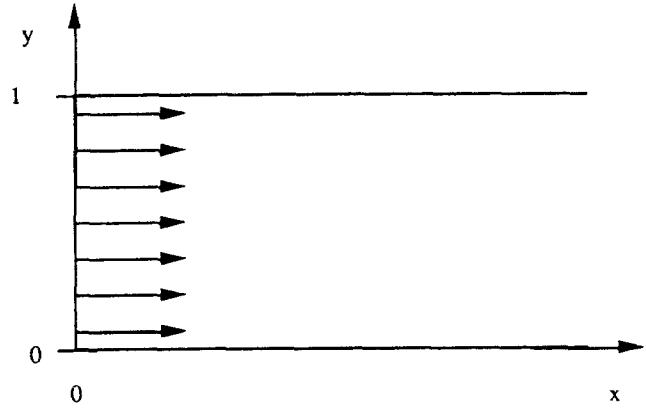

Fig. 1. Inflow.

negative real part. Therefore α_{a2} and α_{b2} are zero by the side condition of Eq. (3.1e), and by Eq. (3.4) with $s=0$ and $V=0$ we get

$$\begin{pmatrix} \hat{u} \\ \hat{v} \\ \hat{p} \end{pmatrix} = \alpha_{a1} \begin{pmatrix} 1 \\ \dfrac{\kappa_{a1}}{i\omega} \\ 0 \end{pmatrix} \cdot e^{-\kappa_{a1} x} + \alpha_{b1} \begin{pmatrix} 1 \\ \dfrac{-i\omega}{\kappa_{b1}} \\ \dfrac{-\kappa_{b1} U - \nu\kappa_{b1}^2 + \nu\omega^2}{\kappa_{b1}} \end{pmatrix} \cdot e^{-\kappa_{b1} x}$$

$$+ \alpha_{b3} \begin{pmatrix} 1 \\ \dfrac{-i\omega}{\kappa_{b3}} \\ \dfrac{-\kappa_{b3} U - \nu\kappa_{b3}^2 + \nu\omega^2}{\kappa_{b3}} \end{pmatrix} \cdot e^{-\kappa_{b3} x} \tag{4.5}$$

The arbitrary constants α_{a1}, α_{b1} and α_{b3} are determined by prescribing three boundary conditions at $x=0$. For $|\omega\nu| \ll 1$ we by Eq. (3.5a) and by Theorem 4.1 have

$$\kappa_{a1} = \frac{\nu\omega^2}{U}(1 + O(\nu^2\omega^2)) \tag{4.6a}$$

$$\kappa_{b1} = \frac{|\omega|}{(1-U^2M^2)^{1/2}}(1 + O(\omega\nu U^3 M^4)) \tag{4.6b}$$

$$\kappa_{b3} = \frac{1-U^2M^2}{U\nu M^2}(1 + O(\omega^2\nu^2 U^4 M^6)) \tag{4.6c}$$

and therefore

$$0 < \kappa_{a1} \ll \kappa_{b1} \ll \kappa_{b3}$$

The eigensolution that corresponds to κ_{b3} represents the very thin boundary layer discovered by Kreiss *et al.* (1991), and the eigensolution corresponding to κ_{b1} represents the boundary layer discovered by Johansson (1991a,b). These boundary layers must be suppressed, which is done by requiring a derivative of high order to be zero at inflow [Johansson (1991a,b,d)]. We suggest to use

$$u(0, y, t) = u_0(y, t) \tag{4.7a}$$

$$\frac{\partial^r v}{\partial x^r}(0, y, t) = 0, \qquad r=0, \text{ or } r=1, \text{ or } r=2 \tag{4.7b}$$

$$\frac{\partial^q u}{\partial x^q}(0, y, t) = 0, \qquad q \geqslant 2 \tag{4.7c}$$

The first condition means that we prescribe an inflow velocity profile for u. The purpose of the second and the third conditions are to suppress the boundary layers.

4.2.1.2. The Suppression of Boundary Layers. Using the Laplace-Fourier transformed version of Eq. (4.7) in Eq. (4.5) together with Eq. (4.6) yields for $q \geqslant \max(r, 1)$

$$\begin{pmatrix} \hat{u} \\ \hat{v} \\ \hat{p} \end{pmatrix} = \frac{\hat{u}_0}{1-\left(\frac{\kappa_{a1}}{|\omega|}\right)^{r+1}} \cdot \left\{ \begin{pmatrix} 1 \\ \frac{\kappa_{a1}}{i\omega} \\ 0 \end{pmatrix} \cdot e^{-\kappa_{a1}x} - \left(\frac{\kappa_{a1}}{|\omega|}\right)^{r+1} \cdot \begin{pmatrix} 1 \\ \frac{-i\omega}{|\omega|} \\ -U \end{pmatrix} \cdot e^{-|\omega|x} \right\} (1+O(M^2)) + \hat{u}_0 \cdot |v\omega M^2|^q \cdot O(|\omega v|^q + |\omega v|^{r+1}) \begin{pmatrix} 1 \\ -i\omega v U M^2 \\ -\frac{1}{UM^2} \end{pmatrix} \cdot e^{-\kappa_{b3}x} \tag{4.8}$$

(See Johansson (1992) for details.) The eigensolution that corresponds to $\kappa_{b1} \approx |\omega|$ represents a boundary layer that has the boundary layer thickness $1/\kappa_{b1} \approx 1/|\omega|$. This layer is suppressed by choosing r large. However, using $r \geqslant 3$ in Eq. (4.7b) will in the time-dependent incompressible case given solutions that grow in time even if the forcing in the system does not, Johansson (1991a,b). We therefore must have $r \leqslant 2$ in the low Mach number case as well. We recommend to use $r = 2$.

The eigensolution that corresponds to κ_{b3} represents the boundary layer with thickness $1/\kappa_{b3} \approx UvM^2$. This layer is efficiently suppressed by choosing q large, and in terms of M it will be $O(M^{2q})$ in u, $O(M^{2q+2})$ in v and $O(M^{2q-2})$ in p. Hence, in order to suppress the p-component of this boundary layer we must have $q \geqslant 2$. We will in the following see that $q \geqslant 2$ is also necessary for the convergence to the true incompressible solution as $M \to 0$. We recommend to use $q = 3$.

4.2.1.3. Convergence to Incompressible Solution as $M \to 0$. In Johansson (1991a,b) the inflow boundary conditions

$$u(0, y, t) = u_0(y, t), \qquad x = 0 \tag{4.9a}$$

$$\frac{\partial^r v}{\partial x^r} = 0, \qquad x = 0, \qquad r = 0, \text{ or } r = 1, \text{ or } r = 2 \tag{4.9b}$$

$$\frac{\partial u}{\partial x} + \frac{\partial v}{\partial y} = 0, \qquad x = 0 \tag{4.9c}$$

were recommended for the incompressible Navier-Stokes equation. The solution on the Laplace-Fourier transform side of the incompressible equation linearized around a constant flow, together with the boundary conditions in Eq. (4.9), is

$$\begin{pmatrix} \hat{u} \\ \hat{v} \\ \hat{p} \end{pmatrix} = \frac{\hat{u}_0}{1 - \left(\frac{\kappa_{a1}}{|\omega|}\right)^{r+1}} \cdot \left\{ \begin{pmatrix} 1 \\ \frac{\kappa_{a1}}{i\omega} \\ 0 \end{pmatrix} \cdot e^{-\kappa_{a1} x} - \left(\frac{\kappa_{a1}}{|\omega|}\right)^{r+1} \cdot \begin{pmatrix} 1 \\ \frac{-i\omega}{|\omega|} \\ -U \end{pmatrix} \cdot e^{-|\omega| x} \right\} \tag{4.10}$$

[see Johansson (1991a,b)]. By letting $M \to 0$ we see that the low Mach number solution of Eq. (4.8) will converge to the true incompressible solution of Eq. (4.10), and that the convergence rate is $O(M^2)$. Hence, the boundary condition in Eq. (4.7) fulfills all the requirements (i)–(iii) in the beginning of Section 4.2.

The requirement $q \geqslant 2$ is necessary for the convergence as $M \to 0$. Letting $q = 1$ and $r = 0$ or $r = 1$, we by Eq. (4.8) see that the p-component of the boundary layer corresponding to κ_{b3} will, as a function of M, be $O(1)$. For every fixed $x > 0$ we as $M \to 0$ still get convergence to Eq. (4.10), but the convergence is not uniform in x.

Letting $q = 1$ and $r = 2$ will be even worse. In this case we in the same way as above get

$$\begin{pmatrix} \hat{u} \\ \hat{v} \\ \hat{p} \end{pmatrix} \to \hat{u}_0 \cdot \begin{pmatrix} 1 \\ \frac{-i\omega}{|\omega|} \\ -U \end{pmatrix} \cdot e^{-|\omega| x}, \qquad \text{as} \quad M \to 0$$

This solution is totally unphysical, as only the boundary layer part corresponding to $\kappa_{b1} \approx |\omega|$ is left in the solution. Furthermore, this solution does not fulfill the boundary condition (4.9b).

Hence, in order to get convergence to the true incompressible solution as $M \to 0$ it is important that the requirement $q \geqslant 2$ is fulfilled.

4.2.2. Outflow

4.2.2.1. The Boundary Condition. (See Fig. 2). Choosing $U<0$ makes $x=0$ an outflow boundary. Furthermore, $U<0$ implies that κ_{a1} and κ_{b1} have a strictly positive real part, whereas κ_{a2}, κ_{b2} and κ_{b3} have a strictly negative real part. Therefore α_{a2}, α_{b2} and α_{b3} are zero by the side condition in Eq. (3.1e), and by Eq. (3.4) with $s=0$ and $V=0$ we get

$$\begin{pmatrix} \hat{u} \\ \hat{v} \\ \hat{p} \end{pmatrix} = \alpha_{a1} \begin{pmatrix} 1 \\ \dfrac{\kappa_{a1}}{i\omega} \\ 0 \end{pmatrix} \cdot e^{-\kappa_{a1} x} + \alpha_{b1} \begin{pmatrix} 1 \\ \dfrac{-i\omega}{\kappa_{b1}} \\ \dfrac{-\kappa_{b1} U - \nu\kappa_{b1}^2 + \nu\omega^2}{\kappa_{b1}} \end{pmatrix} \cdot e^{-\kappa_{b1} x} \tag{4.11}$$

The two arbitrary constants α_{a1} and α_{b1} are determined by prescribing two boundary conditions.

For $|\omega\nu| \ll 1$ we by Eq. (3.5a) and Theorem 4.1 have

$$\kappa_{a1} = \frac{|U|}{\nu}(1 + O(\nu^2\omega^2 U^{-2})) \tag{4.12a}$$

$$\kappa_{b1} = \frac{|\omega|}{(1-U^2M^2)^{1/2}}(1 + O(\omega\nu U^3 M^4)) \tag{4.12b}$$

and therefore

$$0 < \kappa_{b1} \ll \kappa_{a1}$$

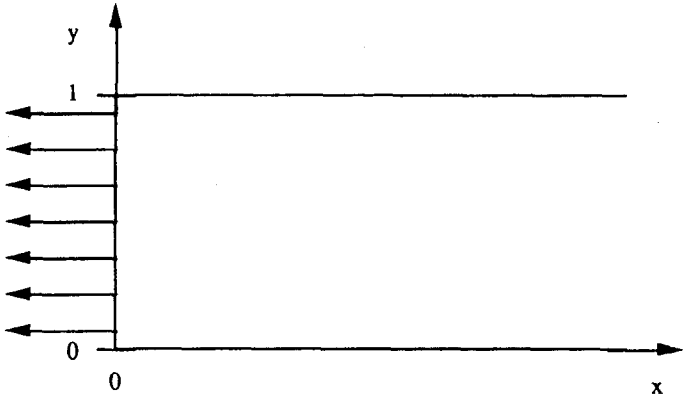

Fig. 2. Outflow.

Hence, the eigensolution that corresponds to κ_{a1} represents the unphysical boundary layer part of the solution, and it must therefore be suppressed. As in the inflow case this is done by requiring a derivative of high order to be zero. We suggest to use

$$p(0, y, t) = p_0(y, t) \tag{4.13a}$$

$$\frac{\partial^k v}{\partial x^k}(0, y, t) = 0, \qquad k \geqslant 1 \tag{4.13b}$$

4.2.2.2. The Suppression of Boundary Layers. Using the Laplace-Fourier transformed version of Eq. (4.13) in Eq. (4.11) together with Eq. (4.12) yields

$$\begin{pmatrix} \hat{u} \\ \hat{v} \\ \hat{p} \end{pmatrix} = -\frac{\hat{p}_0}{U} \cdot \left\{ -\left(\frac{|\omega|}{\kappa_{a1}}\right)^k \begin{pmatrix} \dfrac{|\omega|}{\kappa_{a1}} \\ \dfrac{|\omega|}{i\omega} \\ 0 \end{pmatrix} \cdot e^{-\kappa_{a1} x} \right.$$

$$\left. + \begin{pmatrix} 1 \\ \dfrac{-i\omega}{|\omega|} \\ -U \end{pmatrix} \cdot e^{-|\omega| x} \right\} (1 + O(M^2)) \tag{4.14}$$

[See Johansson (1992) for details.] As by Eq. (4.12) $|\omega|/\kappa_{a1} \approx \nu\, |\omega|/|U| \ll 1$ we see that the larger the k we choose, the more suppressed the boundary layer will be. Furthermore, we must choose $k \geqslant 1$, otherwise the boundary layer part in the v-component will be $O(1)$. We recommend to use $k = 2$.

4.2.2.3. Convergence to Incompressible Solution as $M \to 0$. In Johansson (1991a,b) the outflow boundary conditions to

$$p(0, y, t) = p_0(y, t) \tag{4.15a}$$

$$\frac{\partial^j u}{\partial x^j}(0, y, t) = 0 \tag{4.15b}$$

$$\frac{\partial^k v}{\partial x^k}(0, y, t) = 0 \tag{4.15c}$$

were recommended for the incompressible Navier-Stokes equation. The solution on the Laplace-Fourier transform side of the incompressible

equation linearized around a constant flow, together with the boundary conditions Eq. (4.15) with $j=k+1$, is

$$\begin{pmatrix}\hat{u}\\ \hat{v}\\ \hat{p}\end{pmatrix} = -\frac{\hat{p}_0}{U}\cdot\left\{-\left(\frac{|\omega|}{\kappa_{a1}}\right)^k\begin{pmatrix}\frac{|\omega|}{\kappa_{a1}}\\ \frac{|\omega|}{i\omega}\\ 0\end{pmatrix}\cdot e^{-\kappa_{a1}x}+\begin{pmatrix}1\\ \frac{-i\omega}{|\omega|}\\ -U\end{pmatrix}\cdot e^{-|\omega|x}\right\} \tag{4.16}$$

[see Johansson (1991a,b)]. By letting $M\to 0$ we see that the low Mach number solution Eq. (4.14) will converge to the true incompressible solution Eq. (4.16), and that the convergence rate is $O(M^2)$.

Hence, the boundary condition Eq. (4.13) fulfills all the requirements (i)–(iii) in the beginning of Section 4.2.

5. SLIP AND NO SLIP BOUNDARY CONDITIONS

In this section we consider (see Fig. 3) the case $U=0$, i.e. the linearization around the solution near a boundary through which no fluid passes. Using Theorem 3.1 and the side condition Eq. (3.1e), the fundamental solution of Eq. (3.1) for $U=0$ becomes

$$\begin{pmatrix}\hat{u}\\ \hat{v}\\ \hat{p}\end{pmatrix} = \alpha_{a1}\begin{pmatrix}1\\ \frac{\kappa_{a1}}{i\omega}\\ 0\end{pmatrix}\cdot e^{-\kappa_{a1}x}+\alpha_{b1}\begin{pmatrix}1\\ \frac{-i\omega}{\kappa_{b1}}\\ \frac{s+i\omega V-\nu\kappa_{b1}^2+\nu\omega^2}{\kappa_{b1}}\end{pmatrix}\cdot e^{-\kappa_{b1}x}$$

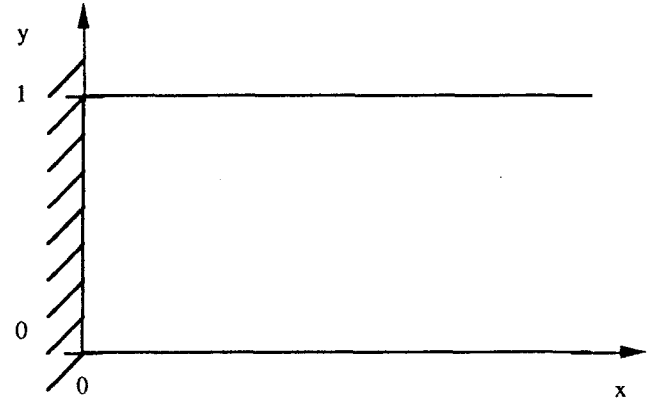

Fig. 3. $U=0$ at $x=0$.

The two arbitrary constants α_{a1} and α_{b1} are determined by prescribing two boundary conditions. We suggest two alternatives. The first is to use the no slip condition for solid wall, i.e. to prescribe the velocities u and v. The second alternative is to prescribe conditions for a free surface which is fixed at $x=0$, i.e. to demand that no fluid passes through the boundary ($u=0$ at $x=0$) and that there is no shear stress at the boundary ($v_x=0$ at $x=0$).

Hence, for $U=0$ we suggest to use

$$u(0, y, t)=0 \tag{5.1a}$$

$$\frac{\partial^r v}{\partial x^r}(0, y, t)=0, \qquad r=0 \text{ or } r=1 \tag{5.1b}$$

6. NUMERICAL RESULTS

In this section we present numerical solutions of the nonlinear time-dependent Navier-Stokes equation for low Mach number flow, formulated as Eq. (1.2). We show that the divergence in the low Mach number solution is $O(M^2)$ and after Richardson extrapolation to $M^2=0$ the divergence is $O(M^4)$. This was predicted by the linear theory and by Kreiss *et al.* (1991). We will show that making one calculation with $M^2=0.1$ and one with $M^2=0.05$ and using Richardson extrapolation to $M^2=0$ yields a solution with very small divergence. As the time step must be chosen approximately such that $\Delta t \cdot (i/(M\,\Delta x)-\nu/\Delta x^2)$ is in the stability region of the method, the restriction on the time step due to the Mach number is not serious, and the equations can be integrated by explicit numerical methods. Hence, integrating Eq. (1.2) with explicit methods for two values of M^2 and using Richardson extrapolation to $M^2=0$, is a very efficient method for solving time-dependent incompressible flow problems. The same technique can be used for computing very low Mach number flow.

6.1. The Numerical Method

We have written a code for solving the time-dependent Navier-Stokes equation for low Mach number flow, formulated as Eq. (1.2). Figure 4 illustrates the calculation domain: $0 \leqslant x \leqslant L$, $0 \leqslant y \leqslant 1$, $0 \leqslant t < \infty$, i.e. a two-dimensional straight channel.

As boundary condition we at $x=0$ apply the inflow condition of Eq. (1.5) with $r=2$ and $q=3$, and at $x=L$ we apply the outflow condition of Eq. (1.6) with $k=2$ and $p_0 \equiv 0$. At the solid walls we apply $u=v=0$.

As initial condition we let $u=v=p=0$.

Equation (1.2) is approximated by the standard fourth order central differences on a Cartesian grid. This means that the differential operators

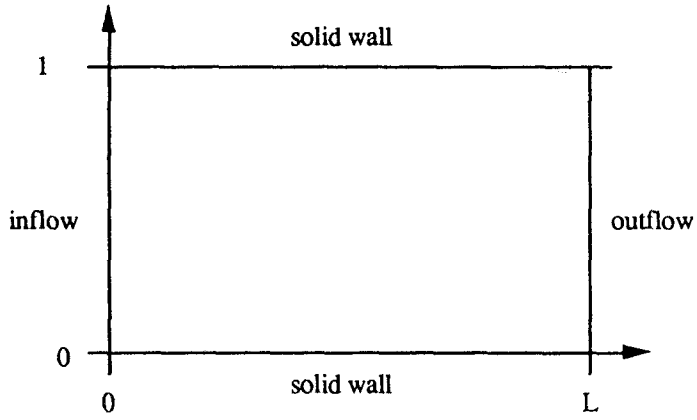

Fig. 4. The calculation domain.

$\partial/\partial x$, $\partial/\partial y$ and $\partial^2/\partial x^2 + \partial^2/\partial y^2$ are exchanged for finite difference operators according to

$$\frac{\partial}{\partial x} \to D_x^{(4)} = D_{0x}\left(I - \frac{\Delta x^2}{6} D_{+x}D_{-x}\right)$$

$$\frac{\partial}{\partial y} \to D_y^{(4)} = D_{0y}\left(I - \frac{\Delta y^2}{6} D_{+y}D_{-y}\right)$$

$$\frac{\partial^2}{\partial x^2} + \frac{\partial^2}{\partial y^2} \to \Delta^{(4)} = D_{+x}D_{-x}\left(I - \frac{\Delta x^2}{12} D_{+x}D_{-x}\right) + D_{+y}D_{-y}\left(I - \frac{\Delta y^2}{12} D_{+y}D_{-y}\right)$$

The superscript (4) in the notation $D_x^{(4)}$, $D_y^{(4)}$ and $\Delta^{(4)}$ is used to indicate that these finite difference operators are fourth order accurate. As the spatial approximation is fourth order accurate, we also need additional boundary conditions to get the method well defined, see Johansson (1991a,b). We use extrapolation of a high order of u, v, and p as extra boundary conditions.

We denote the so derived approximation of the velocity and pressure $\begin{pmatrix} u \\ v \\ p \end{pmatrix}(x_i, y_j, t)$ by $w_{i,j}(t)$ and the vector consisting of the $w_{i,j}$:s in all gridpoints (i, j) by $\underline{w}$. The method of lines approximation of Eq. (1.2) can then be written as

$$\underline{w}_t = F(\underline{w}) \tag{6.1}$$

This system of nonlinear ordinary differential equations is solved by integrating in time with the 4:th order Adams-Bashforth-Moulton predictor-corrector method, ABM4, i.e., the Adams-Bashforth 3:rd order method is used in the predictor step, and the Adams-Moulton 4:th order method is used in the corrector step. Hence, the Eq. (6.1) is integrated by

$$\underline{w}^{n+1/2} = \underline{w}^n + \frac{\Delta t}{12}(23F(\underline{w}^n) - 16F(\underline{w}^{n-1}) + 5F(\underline{w}^{n-2})) \qquad \text{(predictor step)}$$

$$\underline{w}^{n+1} = \underline{w}^n + \frac{\Delta t}{24}(9F(\underline{w}^{n+1/2}) + 19F(\underline{w}^n) - 5F(\underline{w}^{n-1}) + F(\underline{w}^{n-2})) \qquad \text{(corrector step)}$$

The time step Δt is chosen so that the numerical solution of the constant coefficient Cauchy problem

$$u_t + UD_x^{(4)}u + VD_y^{(4)}u - \nu\,\Delta^{(4)}u + D_x^{(4)}p = 0$$
$$v_t + UD_x^{(4)}v + VD_y^{(4)}v - \nu\,\Delta^{(4)}v + D_y^{(4)}p = 0$$
$$p_t + UD_x^{(4)}p + VD_y^{(4)}p + M^{-2}\cdot(D_x^{(4)}u + D_y^{(4)}v) = 0$$

by integrating in time with ABM4 is stable. This means that if $\min(\Delta x, \Delta y)/(\nu M) \gg 1$, we must choose Δt such that

$$i\cdot\Delta t\cdot 1.372\cdot\left(\frac{|U|}{\Delta x} + \frac{|V|}{\Delta y} + M^{-1}\left(\frac{1}{\Delta x^2} + \frac{1}{\Delta y^2}\right)^{1/2}\right) - \Delta t\cdot\frac{16\nu}{3}\left(\frac{1}{\Delta x^2} + \frac{1}{\Delta y^2}\right)$$

is in the stability region of ABM4 [Johansson (1992)].

On the other hand, if $\min(\Delta x, \Delta y)/(\nu M) \ll 1$, it is sufficient to choose Δt such that

$$i\cdot\Delta t\cdot 1.372\cdot\left(\frac{|U|}{\Delta x} + \frac{|V|}{\Delta y}\right) - \Delta t\cdot\frac{16\nu}{3}\left(\frac{1}{\Delta x^2} + \frac{1}{\Delta y^2}\right)$$

is in the stability region of ABM4 [Johansson (1992)].

6.2. The Test Cases

The different test cases are defined by the choice of the inflow velocity profile $u_0(y, t)$ in the boundary condition of Eq. (1.5). We let

$$u_0(y, t) = \{u_{0\text{stat}}(y) + u_{0\varepsilon}(y)\cdot\sin(\pi t/2)\}\cdot\psi(t) \qquad \text{(6.2a)}$$

where

$$\psi(t)=\begin{cases}0, & t\leqslant 0\\ \dfrac{1}{1+\exp\left(\dfrac{3}{t-3}+\dfrac{3}{t}\right)}, & 0<t<3\\ 1, & t\geqslant 3\end{cases} \tag{6.2b}$$

The function $u_{0\text{stat}}$ in Eq. (6.2a) is plotted in Fig. 5.

We have used three alternatives for the function $u_{0\varepsilon}$ in Eq. (6.2a). The first is to let $u_{0\varepsilon}$ be identically zero, the second is to let $u_{0\varepsilon}$ be antisymmetric around $y=\frac{1}{2}$ and the third is to let $u_{0\varepsilon}$ be symmetric around $y=\frac{1}{2}$. The antisymmetric and symmetric alternatives are shown in Figs. 6a and 6b, respectively.

The function ψ in Eqs. (6.2a) and (6.2b) obtains its final value at $t=3$. Note that $\psi\in C^{\infty}(-\infty,\infty)$ and that $(d^j\psi/dt^j)(0)=0$ for all $j\geqslant 0$. As the initial value vanishes identically and as the forcing function is smooth, the generation of sound waves (i.e. fast oscillations in time) will be small, Kreiss *et al.* (1991). However, it is also important that ψ and a couple of its derivatives are $O(1)$ for all t. To see how well this criterion is fulfilled we in Fig. 7 plot ψ and its first three derivatives.

Both ψ, ψ', and ψ'' are bounded by 1.1, whereas ψ''' is bounded by 4. If we try to make the start up time shorter than 3, the derivatives will

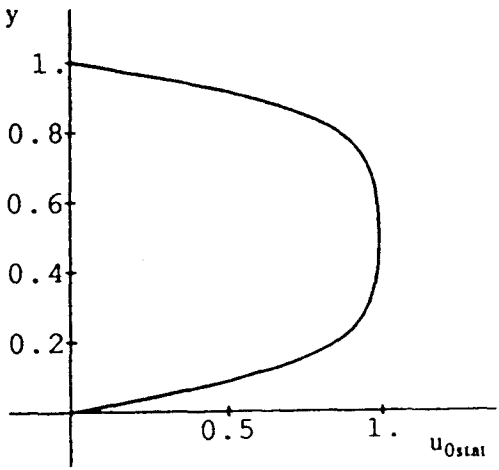

Fig. 5

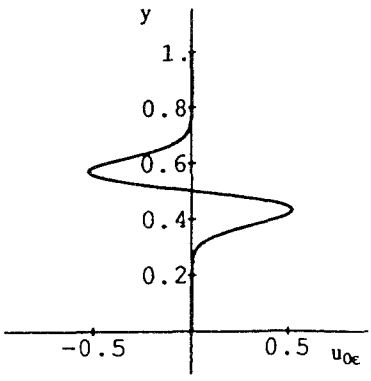

Fig. 6a. $u_{0\varepsilon}$, the antisymmetric case.

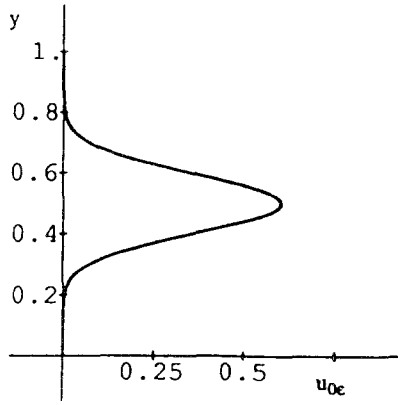

Fig. 6b. $u_{0\varepsilon}$, the symmetric case.

be larger. Numerical tests showed that using the start up time 3 was a satisfactory compromise between short start up time and small value of the derivatives of ψ.

6.3. Results. Convergence as $M \to 0$

We now present the result of calculations with different inflow profiles and different Mach numbers. In all calculations the flow is started from rest

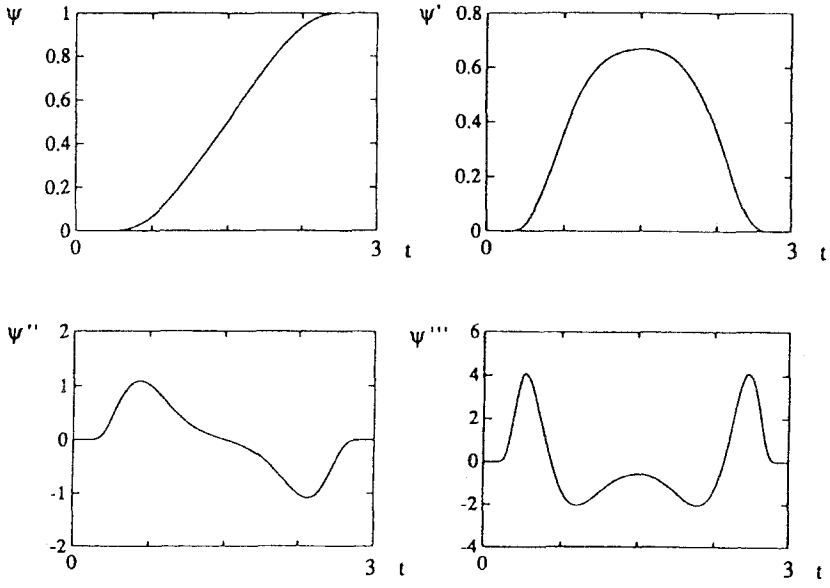

Fig. 7. ψ, ψ', ψ'' and ψ'''.

and it is driven by the time dependent inflow velocity profile $u_0(y, t)$. In the first case we reach steady state, whereas we in the second case let the inflow velocity profile for $t \geqslant 3$ be periodic in time. The calculations are carried through for $\nu = 0.05$ and for four different values of M^2, namely

$$M^2 = 0.2$$

$$M^2 = 0.1$$

$$M^2 = 0.05$$

and

$$M^2 = 0.025$$

We let the channel length $L = 1.25$ and we use 50 points in the x-direction and 42 in the y-direction.

6.3.1. $u_{0\varepsilon} \equiv 0$, *that is Convergence to Steady State*

In the first case we let

$$u_0(y, t) = u_{0\text{stat}}(y) \cdot \psi(t)$$

This means that $u_0(y, t)$ reaches its final value at $t = 3$.

In order to see how fast steady state is reached, and how small the divergence is at steady state, we plot the maximum value of the divergence as a function of time. In Fig. 8a we show the maximal divergence in the channel as a function of t and in Fig. 8b we show the same thing, but after Richardson extrapolation. We see that the divergence has a peak at about $t = 3$ and that steady state is reached at about $t = 7$.

In Fig. 8c and Table I we show the maximal divergence at $t = 10$ (i.e. at steady state) as a function of M^2. In Fig. 8d and Table I we show the same thing, but after Richardson extrapolation.

Table I. The Maximal Divergence at $t = 10$, i.e. at Steady State

M^2	Maximal divergence no extrapolation	Maximal divergence after extrapolation
0.200	0.218	0.070
0.100	0.081	0.011
0.050	0.039	0.0025
0.025	0.019	

See Figs. 8c and 8d.

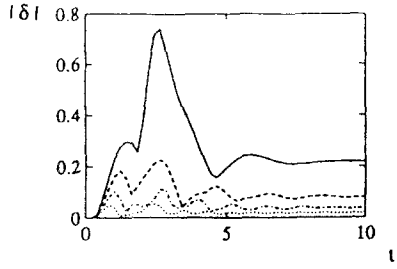

Figure 8.a

$\max_{\substack{0\le x\le L\\ 0\le y\le 1}} |\delta(x,y,t,M^2)|$

——: M^2=0.2
------: M^2=0.1
-·-·-: M^2=0.05
·····: M^2=0.025

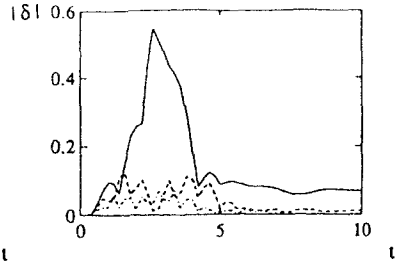

Figure 8.b

$\max_{\substack{0\le x\le L\\ 0\le y\le 1}} |\delta(x,y,t,2M^2) - 2\cdot\delta(x,y,t,M^2)|$

——: M^2=0.1
------: M^2=0.05
-·-·-: M^2=0.025

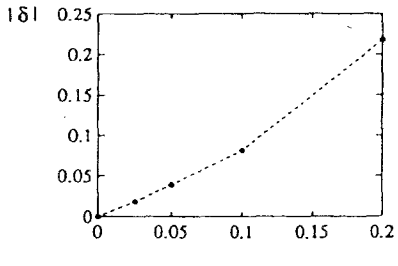

Figure 8.c

$\max_{\substack{0\le x\le L\\ 0\le y\le 1}} |\delta(x,y,10,M^2)|$

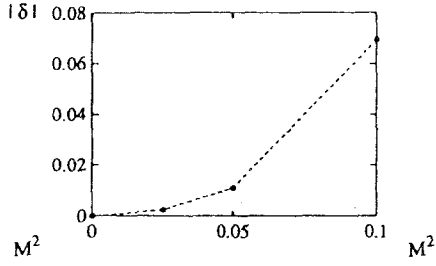

Figure 8.d

$\max_{\substack{0\le x\le L\\ 0\le y\le 1}} |\delta(x,y,10,2M^2) - 2\cdot\delta(x,y,10,M^2)|$

Fig. 8. The effect of Richardson extrapolation when $u_{0_\varepsilon} \equiv 0$, i.e. convergence to steady state. See Section 6.3.1 for further explanations.

We clearly see that the maximal divergence is proportional to M^2. After Richardson extrapolation the maximal divergence is approximately proportional to M^4. Furthermore, making two calculations, one with $M^2 = 0.100$ and one with $M^2 = 0.050$, and applying Richardson extrapolation yields a maximal divergence of 0.011. This is smaller than if one calculation with $M^2 = 0.025$ is made. By applying Richardson extrapolation on the results of the calculations with $M^2 = 0.050$ and $M^2 = 0.025$, we make the divergence decrease by a factor $0.019/0.0025 = 7.6$, compared to only using the result of the calculation with $M^2 = 0.025$.

6.3.2. $u_{0\varepsilon} \neq 0$, *that is the Inflow Profile is Periodic in Time*

In the second case we let

$$u_0(y, t) = \{u_{0\text{stat}}(y) + u_{0\varepsilon}(y) \cdot \sin(\pi t/2)\} \cdot \psi(t)$$

where $u_{0\varepsilon}$ is either of the functions shown in Fig. 6. This means that we start the flow in a similar way as was done in the first case. However, we now also have a periodic $O(1)$ disturbance $u_{0\varepsilon}(y) \cdot \sin(\pi t/2)$ in the inflow forcing function $u_0(y, t)$.

In order to see how small the divergence is when $u_{0\varepsilon}$ is the antisymmetric function in Fig. 6a, we plot the maximum value of the divergence as a function of time. In Fig. 9a we show the time development of the maximal divergence in the channel for t so large that the flow has become periodic. We show the result for one period. In Fig. 9b we see the same thing, but after Richardson extrapolation. The divergence attains its maximum at $t = 11$ and $t = 13$, i.e. at the same values of t for which the inflow profile reaches its maximum.

In Fig. 9c and Table II we show the maximum of the divergence over

Table II. The Maximal Divergence Over One Period When $u_{0\varepsilon}$ is the Antisymmetric Function[a]

M^2	Maximal divergence no extrapolation	Maximal divergence after extrapolation
0.200	1.266	
0.100	0.528	0.209
0.050	0.240	0.049
0.025	0.115	0.010

[a] See Fig. 6a and Figs. 9c and 9d.

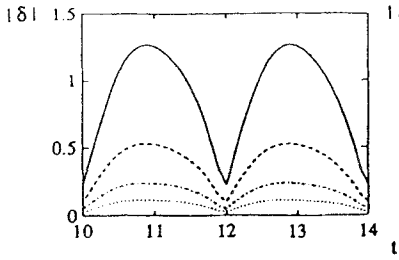

Figure 9.a

$\max_{\substack{0\le x\le L\\ 0\le y\le 1}} |\delta(x,y,t,M^2)|$

——: M^2=0.2
------: M^2=0.1
-·-·-: M^2=0.05
·····: M^2=0.025

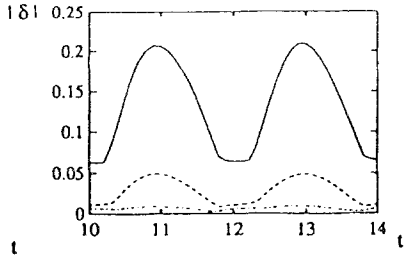

Figure 9.b

$\max_{\substack{0\le x\le L\\ 0\le y\le 1}} |\delta(x,y,t,2M^2) - 2\cdot\delta(x,y,t,M^2)|$

——: M^2=0.1
------: M^2=0.05
-·-·-: M^2=0.025

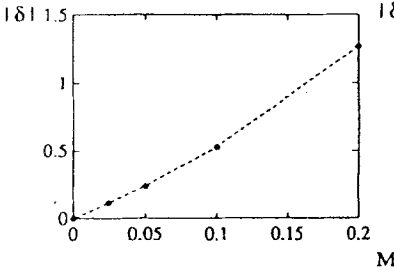

Figure 9.c

$\max_{\substack{0\le x\le L\\ 0\le y\le 1\\ 10\le t\le 14}} |\delta(x,y,t,M^2)|$

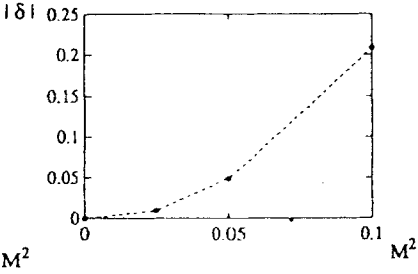

Figure 9.d

$\max_{\substack{0\le x\le L\\ 0\le y\le 1\\ 10\le t\le 14}} |\delta(x,y,t,2M^2) - 2\cdot\delta(x,y,t,M^2)|$

Fig. 9. The effect of Richardson extrapolation when u_{0_E} equals the function in Fig. 6a, i.e. the inflow velocity profile contains a part that is periodic in time and antisymmetric around $y = 0.5$. See Section 6.3.2 for further explanations.

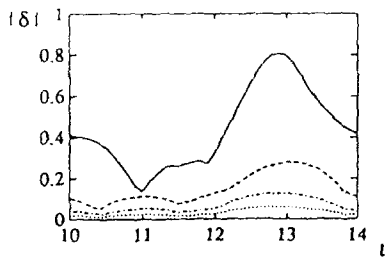

Figure 10.a

$\max_{\substack{0\le x\le L\\ 0\le y\le 1}} |\delta(x,y,t,M^2)|$

——: M^2=0.2
------: M^2=0.1
-·-·-: M^2=0.05
·····: M^2=0.025

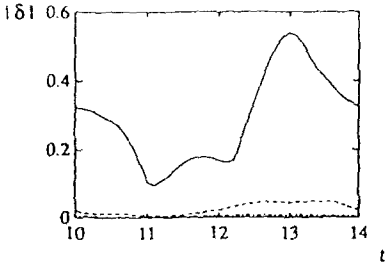

Figure 10.b

$\max_{\substack{0\le x\le L\\ 0\le y\le 1}} |\delta(x,y,t,2M^2) - 2\cdot\delta(x,y,t,M^2)|$

——: M^2=0.1
------: M^2=0.05
-·-·-: M^2=0.025

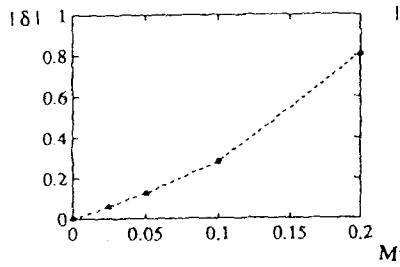

Figure 10.c

$\max_{\substack{0\le x\le L\\ 0\le y\le 1\\ 10\le t\le 14}} |\delta(x,y,t,M^2)|$

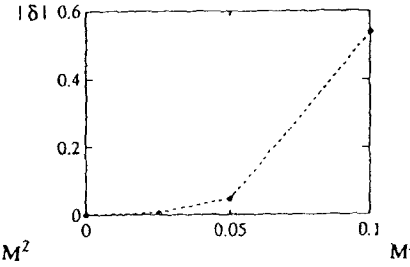

Figure 10.d

$\max_{\substack{0\le x\le L\\ 0\le y\le 1\\ 10\le t\le 14}} |\delta(x,y,t,2M^2) - 2\cdot\delta(x,y,t,M^2)|$

Fig. 10. The effect of Richardson extrapolation when u_{0_E} equals the function in Fig. 6b, i.e. the inflow velocity profile contains a part that is periodic in time and symmetric around $y = 0.5$. See Section 6.3.2 for further explanations.

Table III. The Maximal Divergence Over One Period When $u_{0\varepsilon}$ is the Symmetric Function[a]

M^2	Maximal divergence no extrapolation	Maximal divergence after extrapolation
0.200	0.809	0.538
0.100	0.281	0.048
0.050	0.127	0.008
0.025	0.060	

[a] See Fig 6b and Figs. 10c and 10d.

one period as a function of M^2. In Fig. 9d and Table II we show the same thing, but after Richardson extrapolation. Note that the divergence is approximately proportional to M^2, and after Richardson extrapolation it is approximately proportional to M^4.

In Fig. 10 and Table III we show the same thing as in Fig. 9 and Table II, but for $u_{0\varepsilon}$ taken to be the symmetric function in Fig. 6b. In Fig. 10a we show the time development of the divergence for t so large that the flow has become periodic in time. We show the result for one period. In Fig. 10b we show the same thing, but after Richardson extrapolation. The divergence attains its maximum at $t = 13$, i.e. at the same value of t for which the inflow profile reaches its maximum.

In Fig. 10c and Table III we show the maximum of the divergence over one period as a function of M^2, and in Fig. 10d and Table III we show the same thing, but after Richardson extrapolation. Note that the divergence is approximately proportional to M^2, and after Richardson extrapolation it is approximately proportional to M^4.

As in Section 6.3.1 we next illustrate the gain of applying Richardson extrapolation to $M^2 = 0$. Making two calculations, one with $M^2 = 0.100$ and one with $M^2 = 0.050$, and applying Richardson extrapolation yields a maximal divergence of 0.049 when $u_{0\varepsilon}$ is antisymmetric, and 0.048 when $u_{0\varepsilon}$ is symmetric. This is smaller than if one calculation with $M^2 = 0.025$ is made. By applying Richardson extrapolation on the results of the calculations with $M^2 = 0.050$ and $M^2 = 0.025$, we make the divergence decrease by a factor $0.115/0.010 = 11.5$ when $u_{0\varepsilon}$ is antisymmetric and by a factor $0.060/0.008 = 7.5$ when $u_{0\varepsilon}$ is symmetric, compared to only using the result of the calculation with $M^2 = 0.025$.

ACKNOWLEDGMENTS

I would like to thank Professor Heinz-Otto Kreiss for initiating this project, and for interesting discussions during the work. I would also like to thank Dr. Jesper Oppelstrup for giving valuable remarks concerning the manuscript.

This project was financed by The Swedish Institute of Applied Mathematics (ITM), NUTEK contract 726-91-01071, TFR contract 91-402 and Navy contract N-00014-83-K-0422. All these contributions are very much appreciated.

REFERENCES

Chorin, A. J. (1967). A numerical method for solving incompressible viscous flow problems, *J. Comput. Phys.* **2**, 12–26.

Dettman, J. W. (1984). *Applied Complex Variables*, Dover Publications, Inc.

Gustafsson, B., Kreiss, H.-O., and Oliger, J. (1990). The approximate solution of time-dependent problems (unpublished manuscript).

Johansson, C. (1991a). Initial-boundary value problems for incompressible fluid flow, Doctoral Thesis in Numerical Analysis, Uppsala University, Department of Scientific Computing, Box 120, S-75104 Uppsala, Sweden.

Johansson, C. (1991b). Boundary conditions for open boundaries for the incompressible Navier-Stokes equation, submitted to *J. Comput. Phys.*, (now published).

Johansson, C. (1991c). Well-posedness in the generalized sense for the incompressible Navier-Stokes equation, *J. Sci. Comput.* **6**(2), 101–127.

Johansson, C. (1991d). Well-posedness in the generalized sense for boundary layer suppressing boundary conditions, *J. Sci. Comput.* **6**(4), 391–414.

Johansson, C. (1992). The numerical solution of low Mach number flow in confined regions by Richardson extrapolation, TRITA-NA-9207. Department of Numerical Analysis and Computing Science, Royal Institute of Technology, NADA, S-100 44 Stockholm, Sweden.

Kreiss, H.-O., and Lorenz, J. (1989). *Initial-Boundary Value Problems and the Navier-Stokes Equations*, Academic Press.

Kreiss, H.-O., Lorenz, J., and Naughton, M. J. (1991). Convergence of the solutions of the compressible to the solutions of the incompressible Navier-Stokes equations, *Adv. Appl. Math.* **12**, 187–214.

Naughton, M. J. (1986). On numerical boundary conditions for the Navier-Stokes equations, Ph.D. thesis, California Institute of Technology, Pasadena, California.